Applied Acoustics 72 (2011) 962–968

Contents lists available at ScienceDirect

Applied Acoustics

journal homepage: www.elsevier.com/locate/apacoust

Coupling transfer matrix method to finite element method for analyzing the acoustics of complex hollow body networks

Fabien Chevillotte [a], Raymond Panneton [b,*]

[a] Matelys – Acoustique et Vibrations, 1 rue Baumer, F69120 Vaulx-en-Velin, France
[b] GAUS, Department of Mechanical Engineering, Université de Sherbrooke (Qc), Canada J1K 2R1

ARTICLE INFO

Article history:
Received 14 January 2011
Received in revised form 20 May 2011
Accepted 8 June 2011
Available online 6 July 2011

Keywords:
Transfer matrix
Admittance matrix
Finite element
Hollow body network
Duct
Sealing part
Noise control

ABSTRACT

This paper exposes a procedure to couple multiport transfer matrices to finite elements for analyzing the acoustics of automotive hollow body networks with a minimum of memory requirements and computational time. Generally, hollow body networks are made up from a series of elongated fluid partitions similar to ducts or waveguides. These fluid partitions generally contain complex elements: junctions, noise control elements, and cavities. The location and type of these elements in the network, mainly the noise control elements (e.g., sealing parts), may impact the noise inside a car. In the proposed hybrid method, the elongated fluid partitions are modeled with fluid finite elements. All complexities are modeled with two-port or multiport transfer matrices. The coupling of these matrices to finite elements is naturally done at the weak integral formulation stage of the acoustical problem. The coupling does not add any degrees of freedom to, nor modify, the original finite element matrix system. Consequently, changing locations and types of noise control elements in the hollow body network is fast and does not require rebuilding the finite element system. This enables optimizing the acoustics of a complex network on a desktop computer. The hybrid method is compared to experimental results on a tee-shaped hollow body networks. Good correlations are obtained.

1. Introduction

The acoustic behavior of automotive hollow body network (HBN) has been recently studied [1,2]. Basically, these networks are made up from waveguides, junctions, and cavities. Nowadays, expanding sealing parts are widely used in HBN. These sealing parts have been inserted to ensure airtightness and waterproofness. These parts are usually made up from expanding foams or an assembly of expanding foams and solid materials (see Fig. 1). One can thus consider four different parts in a HBN. The use of sealing parts has demonstrated an efficient influence on the noise inside car [1,2]. Considering the cost of such parts, the optimization of their types and positions seems to be relevant. It would be of interest to use a numerical model. Unfortunately, the computational time (CPU) and memory allocation of a complete 3D model of the hollow body network of a car are significant. The aim of this work is to find a way to reduce CPU and memory requirements to enable the optimization of realistic hollow body networks.

Recently, Kirby [3] introduced a hybrid numerical method for reducing the number of degrees of freedom in the analysis of an infinitely long duct, where a complex element is placed centrally. The duct is modeled using a wave base modal solution and only the complex element is modeled with finite elements. This modal solution is coupled to finite elements through the use of a point matching or point collocation approach. This hybrid method is efficient and can be generalized to more than one complex element. However, for optimizing the types and positions of complex parts in a network, modeling the complex parts with finite elements, rebuilding and solving the matrix system may be prohibitive in terms of CPU time and memory allocation.

A similar approach was previously proposed by Craggs [4] to study the acoustics of ducts. In his work, Craggs combines the use of finite element stiffness matrix with transfer matrix. Here, the ducts are modeled using transfer matrices then converted into stiffness matrices and assembled to the global finite element stiffness matrix of the system. Again, as in the work by Kirby, the complex parts are modeled with finite elements while applying a dynamic condensation of the stiffness matrix of the complex parts, a substantial reduction in degrees of freedom can be obtained.

In the literature, a huge number of works have been published on the modeling of two-port systems by the transfer matrix method. In acoustics, this powerful method has been applied notably to noise barriers made of a succession of different kinds of materials [5] (solid layer, resistive screen, perforated plate, poroelastic material), mufflers [6–8], expansion chambers [8,9], curved ducts [9], *n*-branch acoustic filters [10]. Also, for these two-port

* Corresponding author.
E-mail address: Raymond.Panneton@USherbrooke.ca (R. Panneton).

0003-682X/$ - see front matter © 2011 Elsevier Ltd. All rights reserved.
doi:10.1016/j.apacoust.2011.06.005

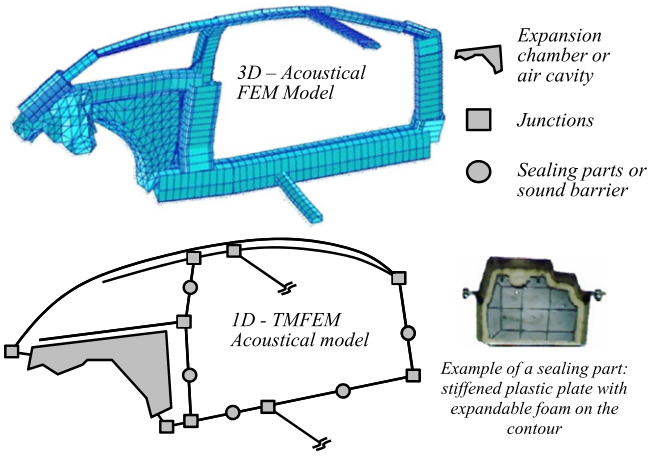

Fig. 1. Hollow body network of a vehicle.

systems, the transfer matrix can be measured experimentally [11,12], or it can be obtained from finite element simulations [4] (mainly in the case where only a virtual CAD model exists).

This paper offers an extension of Cragg's works by naturally coupling the transfer matrix formulation to the weak integral form of the acoustical problem. As presented above, one can easily build a library of transfer matrices for different types of complex parts. Consequently, in the proposed approach, and contrary to previous works, all the complex parts of the HBN are modeled with two-port or multiport transfer matrices, and only the waveguides are modeled with finite elements (see Fig. 1). Consequently, the size of the finite element system (i.e., number of degrees of freedom) is only determined by the mesh of the waveguides; it depends neither on the number nor on kind of complex parts. Besides, the relocation or the addition of complex parts in the HBN does not require rebuilding the finite element system.

In the presented work, only the first propagation mode will be considered (i.e., plane wave mode) as it is the one contributing the most to noise in hollow body networks [3]. In this case, only one-dimensional fluid finite elements will be used and the solution will be valid up to the first cut-off frequency of the network. However, the method can be extended to higher propagation modes using 3D finite element in a manner similar to Craggs [4].

2. Theory

2.1. Statement of the problem

The problem under consideration is presented in Fig. 2. It consists of a hollow body network (HBN) made of elongated fluid partitions (in white) coupled to two-port or multiport acoustical elements (in gray) and to boundary conditions. Examples of two-port elements are expansion chambers, mufflers, porous layers, foam plugs, sealing parts, and noise barriers. Examples of multiport elements are multi-connection junctions, and cavities with multiple input/output branches. In this study, the vibrations of the hollow body network's walls are neglected. The fluid domain Ω is bounded by hard surfaces Γ and the impedance surfaces Γ_e. A noise source is applied at the input surface. Each elongated fluid partition is similar to a waveguide, where it is assumed that only plane waves propagate. This assumption is valid up to the cut-off frequency of the waveguide (i.e., valid for wavelength much smaller than the largest cross-section dimension D). In Fig. 2, one can note that each acoustical element of the HBN is sandwiched between extra fluid layers, the whole forming a shaded zone. In the near field of a part, the plane wave assumption may not hold due to evanescent waves. This is why extra fluid lengths equal to D are added upstream and downstream each acoustical element. This allows evanescent waves to vanish.

2.2. Governing equation in the fluid domain

The field variable in the fluid domain Ω is the acoustical pressure p. Assuming linear acoustics with $\exp(j\omega t)$ time dependence and one-directional sound propagation, the acoustic pressure in each elongated fluid partition is governed by the one-dimensional Helmholtz's equation.

$$\frac{1}{\omega^2\rho_0}\frac{\partial^2 p}{\partial x^2}+\frac{1}{K_a}p=0, \tag{1}$$

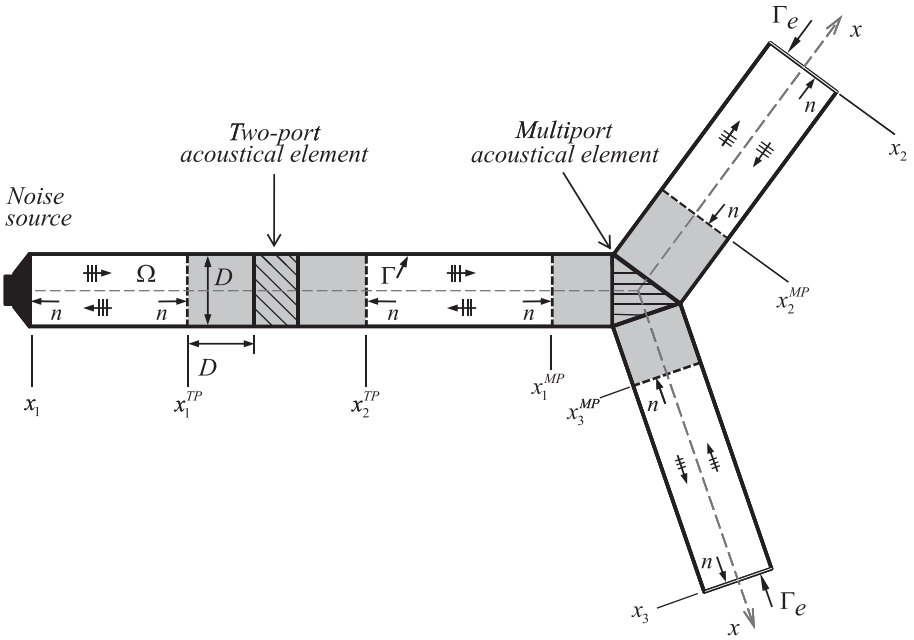

Fig. 2. Geometry of the problem.

where ρ_0 and K_a are respectively the density and adiabatic bulk modulus of the fluid, x is axis of the partition, and ω is angular frequency. In this case, a finite element implementation of Eq. (1) will only use one-dimensional fluid finite elements.

2.3. Transfer matrix for two-port elements

Contrary to the elongated fluid partitions, the acoustical elements of the HBN cannot be generally modeled with one-dimensional elements. However, the transfer matrix method can be used to model the acoustical elements with their extra input and output fluid layers. In the case of a two-port element, the transfer matrix is used to link the acoustical pressures and normal volume flow rates (q_n) on both ports of the element. Assuming normal incidence acoustic plane waves at the input and output ports (dashed lines at x_1^{TP} and x_2^{TP} in Fig. 2), the transfer matrix relation is

$$\begin{Bmatrix} p(x_1^{TP}) \\ q_n(x_1^{TP}) \end{Bmatrix} = \mathbf{Q} \begin{Bmatrix} p(x_2^{TP}) \\ q_n(x_2^{TP}) \end{Bmatrix}, \tag{2}$$

where $\mathbf{Q}$ is the transfer matrix given by

$$\mathbf{Q} = \begin{bmatrix} Q_{11} & Q_{12} \\ Q_{21} & Q_{22} \end{bmatrix}. \tag{3}$$

Following the reciprocity principle [13], the determinant of $\mathbf{Q}$ is equal to -1. The minus sign comes from the fact that the normal components are used. Here, working with volume flow rate is more general than working with velocity since it is not limited to situations where input and output ports have the same cross-section area. Also, as it will be shown, it makes the coupling between the transfer matrix method and the finite element method natural.

For an eventual finite element implementation, the admittance matrix of the two-port acoustical element is more suitable. Consequently, the transfer matrix relation given in Eq. (2) can be rewritten as

$$\begin{Bmatrix} q_n(x_1^{TP}) \\ q_n(x_2^{TP}) \end{Bmatrix} = \mathbf{A}_{TP} \begin{Bmatrix} p(x_1^{TP}) \\ p(x_2^{TP}) \end{Bmatrix}, \tag{4}$$

with the symmetrical admittance matrix given by

$$\mathbf{A}_{TP} = \frac{1}{Q_{12}} \begin{bmatrix} Q_{22} & 1 \\ 1 & -Q_{11} \end{bmatrix}. \tag{5}$$

Note that in the previous equations, the normal volume flow rate is defined by $q_n(x_i) = q(x_i)n(x_i)$, where $q(x_i)$ is the volume flow rate field and $n(x_i)$ is unit normal directed outward to the fluid domain at surface x_i.

The coefficients of matrix $\mathbf{A}$ are usually complex and frequency dependent. For simple acoustical elements (e.g., rigid porous layers or expansion chambers), they can be calculated analytically (see Appendix A). However, for complex elements, they can be obtained experimentally or from three-dimensional finite element simulations (see Appendix A).

2.4. Admittance matrix for multiport elements

Based on the previous section, one can extend the admittance matrix relation to multiport acoustical elements. In this case, the general admittance matrix relation between acoustical pressures and normal volume flow rates at the connection points of a multiport element is

$$\{q_n\}_{MP} = \mathbf{A}_{MP}\{p\}_{MP}, \tag{6}$$

where $\mathbf{A}_{MP}$ is the multiport admittance matrix, and $\{q_n\}_{MP}$ and $\{p\}_{MP}$ are vectors containing the acoustical normal volume flow rates and pressures at the input/output ports of the multiport element (i.e., at the x_i^{MP} positions). Then, Eq. (4) is simply a particular case of Eq. (6) when the acoustical element contains only two ports. Note that from Eq. (6), defining one face as the input port, one can write a multiport transfer matrix similar to Eq. (3); however, this multiport transfer matrix would not be square.

2.5. Weak integral formulation

The Galerkin's procedure applied on Eq. (1) yields the symmetric weak integral formulation [14] of the acoustical problem shown in Fig. 2. Using the one-dimensional linear Euler's equation (i.e., $\rho_0 \partial q/\partial t = -S\partial p/dx$), the weak integral formulation can be written as

$$\int_\Omega \left(\frac{\partial \delta p}{\partial x} \frac{1}{\omega^2 \rho_0} \frac{\partial p}{\partial x} - \delta p \frac{1}{K_a} p \right) S\,dx + j\frac{1}{\omega} \sum_{x_i x_i^{TP} x_i^{MP}} (n q \delta p) = 0, \tag{7}$$

where δp is an admissible variation of the acoustical pressure, and S is cross-section area. Substituting Eqs. (4) and (6) into Eq. (7), the weak integral formulation of the problem can be rewritten as

$$\int_\Omega \left(\frac{\partial \delta p}{\partial x} \frac{1}{\omega^2 \rho_0} \frac{\partial p}{\partial x} - \delta p \frac{1}{K_a} p \right) S\,dx + j\frac{1}{\omega} \left(\sum_{k=TP,MP} \{\delta p\}_k^T \mathbf{A}_k \{p\}_k + \sum_{x_i} (nq\delta p) \right) = 0, \tag{8}$$

It is worth recalling that the admittance matrix $\mathbf{A}_k$ is symmetric due to the reciprocity principle inherent to the variational principle behind the integral formulation. Also, it is worth mentioning that the last term in Eq. (8) is related to the boundary conditions at the input and output surfaces of the HBN, where Dirichlet, Neumann or mixed boundary conditions can be imposed.

Finally, Eq. (8) is general and can be applied to any rigid hollow body network containing one or many different types of acoustical elements below the lowest cut-off frequency of the elongated fluid partitions (or waveguides).

2.6. Finite element implementation

In the presented work, the weak formulation Eq. (8) is discretized using one-dimensional fluid finite element with one degree of freedom per node: the acoustical pressure. Accordingly, within a finite element, it is assumed that the pressure field can be interpolated as

$$p^e = \{N\}^{\mathrm{T}} \{p_n\}^e, \tag{9}$$

where $\{N\}$ is the element's shape function used to approximate the pressure field within element "e", and $\{p_n\}^e$ is the element nodal pressure vector. Substituting Eq. (9) into Eq. (8), the first three terms of the integral formulation give

$$\begin{aligned} &\int_\Omega \frac{\partial \delta p}{\partial x} \frac{1}{\rho_0} \frac{\partial p}{\partial x} S\,dx \Rightarrow \{\delta p_n\}^T \mathbf{K} \{\delta p_n\}, \\ &\int_\Omega \delta p \frac{1}{K_a} p S\,dx \Rightarrow \{\delta p_n\}^T \mathbf{M} \{\delta p_n\}, \\ &\{\delta p\}_k^T \mathbf{A}_k \{p\}_k \Rightarrow \{\delta p\}_k^T \mathbf{A}_k \{p\}_k, \end{aligned} \tag{10}$$

where $\{p_n\}$ represents the global nodal pressure variables, and $\mathbf{K}$ and $\mathbf{M}$ represent the kinetic and compression energy matrices. It is noted that the third term remains unchanged since its pressure vector already contains nodal pressures. Note finally that the discretization of the last term of the integral formulation depends on the boundary conditions applied to the system.

By substituting Eq. (10) into Eq. (8), the following finite element system is formed for the hollow body network:

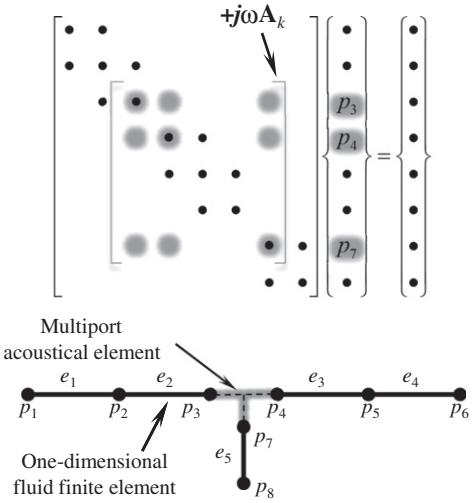

Fig. 3. Assembling of the admittance matrix in the original finite element system.

$$(\mathbf{K}-\omega^2\mathbf{M})\{p_n\}+j\omega\sum_{k=1}^{N}\mathbf{A}_k\{p\}_k=j\omega\{q_n\}, \tag{11}$$

where k denotes this time the kth acoustical element, N is the number of acoustical elements in the HBN, and $\{q_n\}$ is injected nodal harmonic volume flow rate vector. If there is no noise source, $\{q_n\}=\{0\}$. If there is a noise source (e.g., loud speaker) at the first node, the first coefficient of $\{q_n\}$ is equal to the imposed harmonic volume flow rate in m^3/s.

In Eq. (11), the way each admittance matrix $\mathbf{A}_k$ is assembled to the system is made in a finite element sense. It simply consists in summing the coefficients of $\mathbf{A}_k$ to the coefficients of the original system at the locations relative to its associated nodal pressures. This procedure is shown for a three-port acoustical element in Fig. 3. As shown, since the coefficients of $\mathbf{A}_k$ are defined only at existing nodal pressures of the fluid domain, adding the acoustical element does not increase the size of the original system.

Since Eq. (11) only uses one-dimensional fluid finite elements and no additional degrees of freedom for the acoustical elements, the presented approach leads to important saving in setup and solution time when simulating the acoustics of a complex hollow body network (e.g., HBN of an automobile – see Fig. 1). This will be demonstrated in the following sections. Also, with these features, moving acoustical elements to other locations in the studied hollow body network is very simple. This eases, for instance, finding the optimal locations of acoustical elements with a view to minimize the acoustical pressure at given positions.

3. Numerical validations

The basic principle of the hybrid one-dimensional finite element – transfer matrix method (TM-FEM) is numerically validated in this section. Firstly, an air-filled tube with a step discontinuity is considered for validating the coupling between the one-dimensional finite element method and a two-port transfer matrix. Then, an air filled tee-shaped hollow body network is considered in order to validate the coupling between the one-dimensional finite element method and a multiport transfer matrix.

3.1. Two-port acoustical element

A 1-m long tube contains a step discontinuity of its cross-section at 0.5 m as shown in Fig. 4. At one end of the tube, a rigid piston imposes a harmonic volume flow rate of $0.0014\ m^3/s$ at 100 Hz which generates plane waves in the tube. At the other end, a hard surface condition is imposed. The tube is vibration-free and filled with air at rest.

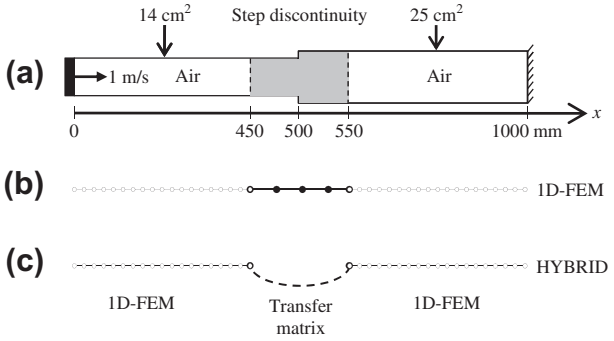

Fig. 4. Two-port validation example (step discontinuity). (a) Geometry model. (b) Full 1D FEM model and (c) hybrid TM-FEM model.

In a first run, the air in the tube is modeled using 25-mm long quadratic one-dimensional fluid finite elements only – see Fig. 4b. The density and bulk modulus of air are $\rho_0=1.21\ kg/m^3$ and $K_a=142{,}272$ Pa, respectively. These properties are used to build matrices **K** and **M** of Eq. (11). In a second run, the zone between 450 and 550 mm is modeled as a two-port transfer matrix – see Fig. 4c. For this simple case, transfer matrix **Q** can be calculated analytically as detailed in Appendix A. Once **Q** is determined, the admittance matrix is built and assembled to the global finite element system. Note that for this simple case, the hybrid TM-FEM model contains 7 degrees-of-freedom less than the full quadratic finite element model.

Fig. 5 compares the amplitude of the pressure field and velocity field calculated at 100 Hz by the two models in function of the position in the tube. One can note the excellent correlation between the full finite element model (FEM) and the hybrid transfer matrix – finite element method (TM-FEM). The thick line in the graph gives the results calculated by the FEM model in the two-port element. The TM-FEM yields no result in this element, except at its input and output ports.

3.2. Multiport acoustical element

The second step of the numerical validation considers a HBN with a multi-connection partition. The tee-shaped HBN presented in Fig. 6 is chosen. Each hollow body zone is made up from a

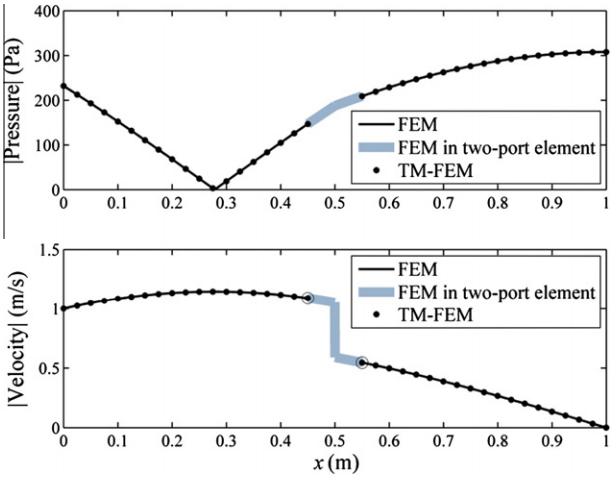

Fig. 5. Numerical validation results on the two-port example. Sound pressure and velocity fields at 100 Hz.

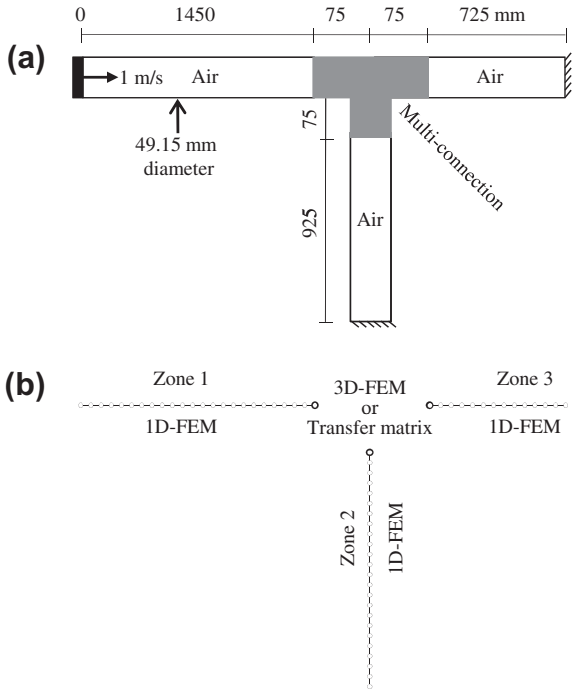

Fig. 6. Multiport validation example (tee-junction). (a) Geometry model and (b) full 1D FEM model or hybrid TM-FEM model.

49.15 mm diameter cylindrical tube. The cut-off frequency for plane waves is 4070 Hz. Three analysis zones are defined on the network. At one end, a volume flow rate is imposed, and hard surface conditions are imposed at the other two ends. The HBN is filled with air with the same properties as defined before. The three waveguides are modeled with 1D quadratic fluid finite elements. A convergence study was performed to ensure convergence of the solution.

In a first run, the connection between the three waveguides is modeled with 3D quadratic fluid finite elements. A particular attention (with Lagrange multipliers) is given to ensure continuity of pressures and volume flow rates at the 1D–3D meshing interfaces. In a second run, the connection is modeled with a multiport admittance matrix. Since the partition has three connections, the matrix is 3×3. In this case, the multiport admittance matrix $\mathbf{A}_{MP}$ is deduced from numerical simulations as detailed in Appendix A. Once $\mathbf{A}_{MP}$ is determined, it is assembled to the global finite element system.

Figs. 7 and 8 respectively compare the mean quadratic sound pressure (L_p) and velocity (L_v) levels calculated by the two models up to 2000 Hz. These quantities are plotted for the three zones. Excellent agreements are obtained between the full FEM results and the hybrid TM-FEM results.

4. Experimental validation

The TM-FEM method is now experimentally tested on the tee-shaped HBN shown in Fig. 9. The length of each zone is given in millimeters. The inner diameter of the tubes is 49.15 mm. A reference microphone is located at the beginning of the first zone, where the acoustic excitation is applied. On the other two terminations, hard surface conditions are applied. Two similar 50-mm thick open-cell melamine foam plugs are inserted in the HBN (one in zone 1 and one in zone 3). Airtight microphone supports are installed on the tubes to measure sound pressure at different positions in the three zones. The measured sound pressure is normalized by the reference microphone.

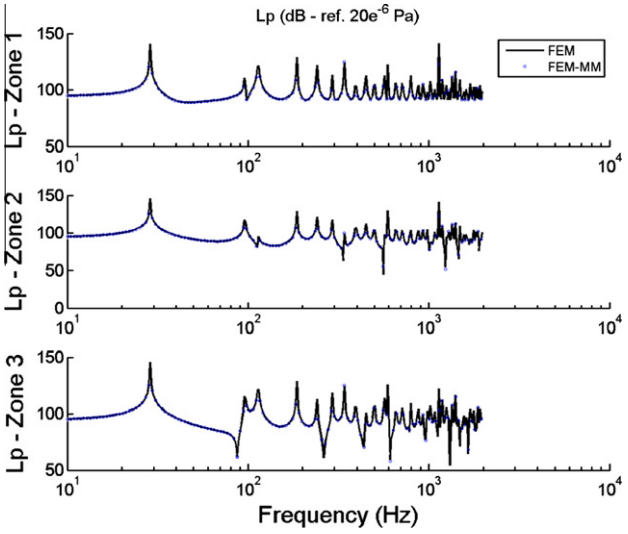

Fig. 7. Numerical validation results on the tee-junction. Mean quadratic sound pressure level in the three zones.

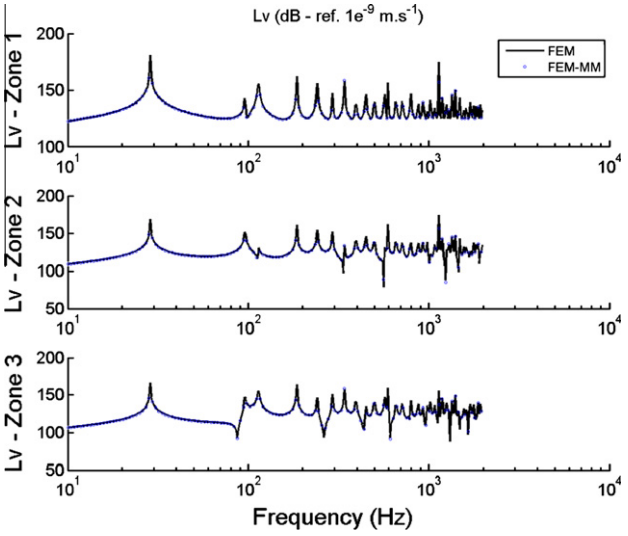

Fig. 8. Numerical validation results on the tee-junction. Mean quadratic sound velocity level in the three zones.

On a numerical viewpoint, the HBN is meshed with quadratic one-dimensional fluid finite elements. Each finite element node fits with a measurement point. Zone 1 contains 29 points, zone 2 contains 20 points, and zone 3 contains 14 points. The multiport admittance matrix of the connection is modeled as detailed in Appendix A. On the other hand, for the sake of simplicity, the two-port admittance matrix of the melamine foam plug is analytically calculated. It is assumed that the foam behaves like an equivalent fluid and its transfer matrix is given by Eq. (A1), with k and Z obtained from the Johnson–Champoux–Allard model as explained in Ref. [5]. The properties of the foam are given elsewhere [15].

Figs. 10 and 11 compare the mean quadratic sound pressure level (in dB-ref pressure at the reference microphone) for each analysis zone without and with the foam plugs, respectively. For both cases, good correlations between the measurements and the simulations are obtained. However, in the case without the foam plugs, one can note that the pressure level is overestimated at the resonances. This difference might be due to the damping of air in narrow tubes (viscous and thermal losses). A damping loss factor of only 0.005 was used for the air in the simulation. Moreover,

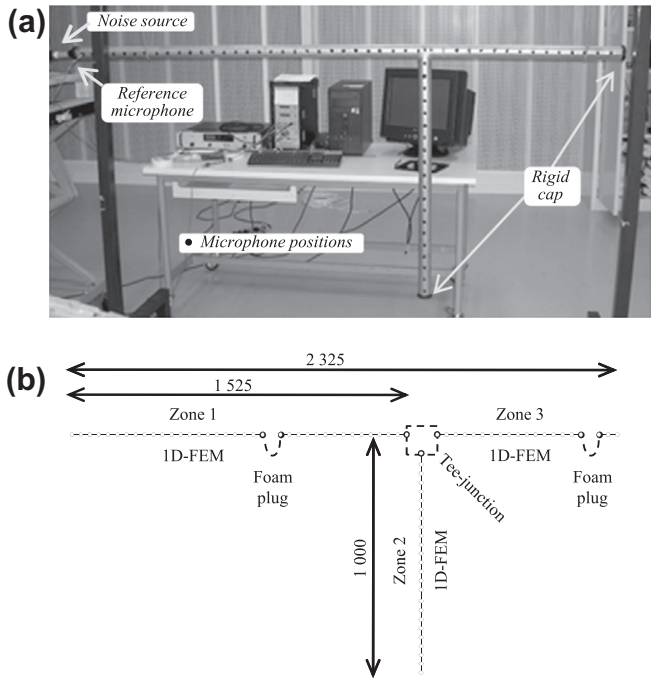

Fig. 9. Experimental setup of a tee-shaped hollow body network containing foam plugs.

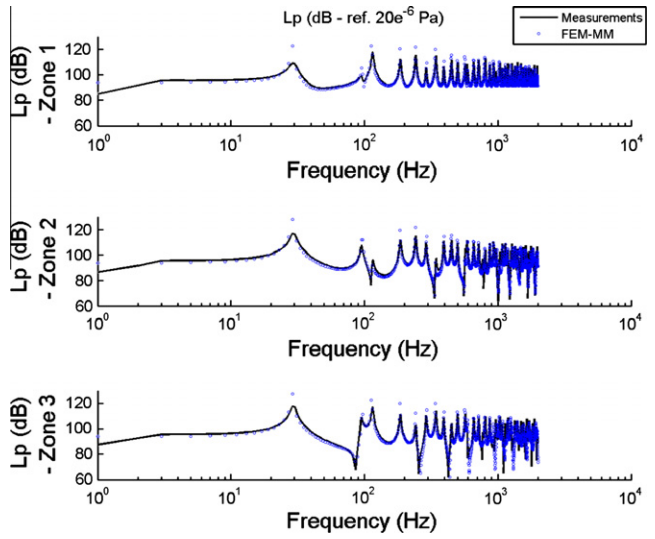

Fig. 10. Experimental validation results on the tee-shaped hollow body network. Case without foam plugs. Mean quadratic sound pressure level.

damping due to the acoustic radiation of the walls exists. This phenomenon was not taken into account in the acoustic model, where the HBN was considered rigid. The overestimation of the pressure level is not visible when the foam plugs are placed into the HBN, see Fig. 11. This is logical since the dissipation due to the foam plugs dominates over the other types of dissipation in this particular HBN. Note that a resonance at 100 Hz of the empty structure in zone 3 has been damped with experimentation but not with the simulation.

The tee-shaped HBN is a simple structure and the number of degrees of freedom can be though significantly reduced by using the hybrid TM-FEM approach. For this particular case, a full converging quadratic 3D model would have approximately 10,000 degrees-of-freedom compared to the 70 degrees-of-freedom of the hybrid model used for the previous simulation. If

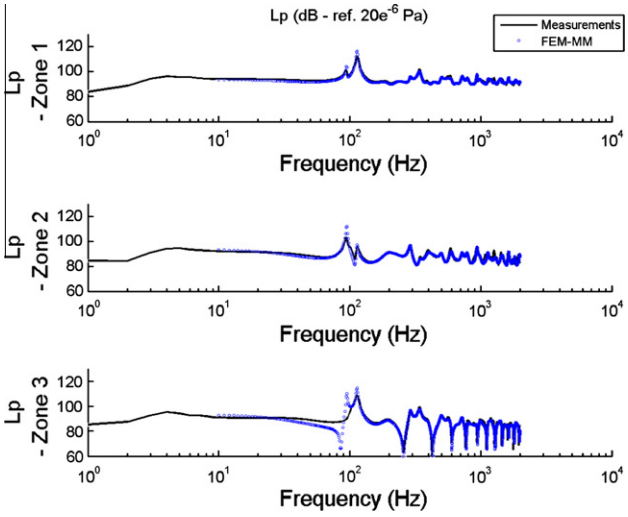

Fig. 11. Experimental validation results on the tee-shaped hollow body network. Case with foam plugs. Mean quadratic sound pressure level.

Table 1
Number of degrees of freedom for three different modeling of the tee-shaped HBN.

Model		Number of degrees of freedom (dof)
Connection (T)	Waveguides	
3D-FEM	3D-FEM	~10,000
3D-FEM	1D-FEM	~470
TM	1D-FEM	~70

only the connection is modeled with 3D finite elements, as done in the previous section, a total of 470 degrees-of-freedom would have been necessary to reach convergence in the analyzed frequency range. These results are summarized in Table 1.

5. Concluding remarks

This work has first presented a hybrid method for coupling transfer matrix and finite element method. The transfer matrix has been expressed in terms of a symmetric elementary admittance matrix to be inserted in the global finite element matrix system. The principle is extended to multiport matrices for coupling multi-connected partitions to finite elements. The basic principles are numerically validated. A correlation with experimentations has been successfully achieved for a simple tee-shaped hollow body network. The method revealed to be very efficient to minimize the number of degrees of freedom, and to reduce CPU time and memory allocation. Future works should consider the addition of airflow in the network to address exhaust system and duct type problems, and extend the method to include higher order propagation modes in a manner similar to the one proposed by Craggs [4].

Acknowledgments

This work was supported by N.S.E.R.C. Canada. Also, the authors wish to thank Henkel Technologies, Christophe Chaut and Jean-Luc Wojtowicki for providing the experimental results.

Appendix A. Determination of admittance matrix

A.1. Simple two-port elements

For simple two-port elements, the admittance matrix $\mathbf{A}_{tp}$ can be obtained analytically. Here, the construction of $\mathbf{A}_{tp}$ is detailed for

the step discontinuity of the cross-section (see Fig. 4). This step discontinuity can be divided into two segments, each having a uniform cross-section area. The length and cross-section area of each segment are (l_1, S_1) and (l_2, S_2), respectively. The acoustic pressures and velocities at both ports of each segment can be modeled with a classical transfer matrix [5]

$$\mathbf{T}_i = \begin{bmatrix} \cos(k_i l_i) & jZ_i \sin(k_i l_i) \\ j\frac{1}{Z_i}\sin(k_i l_i) & \cos(k_i l_i) \end{bmatrix}, \tag{A1}$$

where Z_i and k_i are the characteristic impedance and wave number of the acoustic medium filling the ith segment. At the interface between the two segments, the relation between pressures and velocities is given by

$$\begin{Bmatrix} p^- \\ v^- \end{Bmatrix} = \mathbf{S}\begin{Bmatrix} p^+ \\ v^+ \end{Bmatrix} = \begin{bmatrix} 1 & 0 \\ 0 & \frac{S_2}{S_1} \end{bmatrix}\begin{Bmatrix} p^+ \\ v^+ \end{Bmatrix}, \tag{A2}$$

where superscripts "−" and "+" denote variables that belong to the first segment and second segment, respectively. Consequently, the global transfer matrix of the partition is given by $\mathbf{T} = \mathbf{T}_1\mathbf{S}\mathbf{T}_2$. If the normal volume velocities are used instead of the acoustic velocities (here $q_n = (v \cdot n)S$), the global transfer matrix is transformed into transfer matrix $\mathbf{Q}$ given by

$$\mathbf{Q} = \begin{bmatrix} T_{11} & -T_{12}/S_2 \\ T_{12}S_1 & -T_{22}S_1/S_2 \end{bmatrix}, \tag{A3}$$

where T_{ij} are the coefficients of the global transfer matrix of the expansion chamber. Following the reciprocity principle, the determinant of $\mathbf{T}$ is equal to 1. This yields the determinant of $\mathbf{Q}$ to be equal to −1. Finally, matrix $\mathbf{Q}$ is used in Eq. (5) for obtaining admittance matrix $\mathbf{A}_{tp}$.

A.2. Complex two-port and multiport elements

For multiport and complex two-port elements, the analytical determination of the admittance matrix is often not possible or difficult. In these cases, it has to be determined experimentally or using 3D or 2D finite element simulations. For complex two-port elements, the global transfer matrix $\mathbf{T}$ of the element can be found experimentally following a similar method that is proposed in Refs. [11,12]. This experimental method can also be simulated using the finite element analysis, and can also be transposed to multiport elements. For instance, for the three-port element shown in Fig. 6 and Eq. (6) is

$$\begin{Bmatrix} q_{1n} \\ q_{2n} \\ q_{3n} \end{Bmatrix} = \begin{bmatrix} A_{11} & A_{12} & A_{13} \\ A_{21} & A_{22} & A_{23} \\ A_{31} & A_{32} & A_{33} \end{bmatrix}\begin{Bmatrix} p_1 \\ p_2 \\ p_3 \end{Bmatrix}. \tag{A4}$$

Using a 3D finite element models of the partition (shade zone in Fig. 6), simulations are done with different boundary conditions to determine the A_{ij} coefficients. Since it was shown that this matrix is symmetric (i.e., $A_{ij} = A_{ji}$), six additional equations are necessary to determine matrix $\mathbf{A}_{MP}$. For example, they can be obtained using only three finite element simulations with the following sets of boundary conditions, respectively,

$$\begin{aligned} &1: p_1 = 1;\ p_2 = 0;\ p_3 = 0 \rightarrow A_{11} = q_1;\ A_{21} = q_2;\ A_{31} = q_3 \\ &2: q_{2n} = 1;\ p_1 = 0;\ p_3 = 0 \rightarrow A_{22} = 1/p_2 \\ &3: q_{3n} = 1;\ p_1 = 0;\ p_2 = 0 \rightarrow A_{33} = 1/p_3. \end{aligned} \tag{A5}$$

This method is general and can be applied to all types of two-port and multiport acoustical elements connected to waveguides and its application can be extended to experimentations. The only constraint is that the pressure and velocity fields have to be uniform on each input and output surfaces to ensure plane wave propagation in the waveguides. This is why additional fluid layers upstream and downstream the acoustical elements are added so that evanescent waves vanish.

An alternative to find the transfer matrix of a complex unit is proposed by Craggs [4]. First, the method requires building the finite element stiffness matrix of the unit. Then, dynamic condensation is used to express the stiffness matrix in terms of pressures and volume flow rates at the input and output surfaces of the unit. Finally, the condensed stiffness matrix is converted into a transfer matrix. Applied in 3D, the method can also deal with higher order modes in the waveguides.

References

[1] Lilley KM, Weber PE. Vehicle acoustics solutions. In: SAE 2003 noise & vibration conference and exhibition (Grand Traverse, MI), Document No. 2003-01-1583. <http://papers.sae.org/>2003-01-1583; 2003.

[2] Wojtowicki JL, Panneton R. Improving the efficiency of sealing parts for hollow body network. In: SAE 2005 noise & vibration conference and exhibition (Grand Traverse, MI), Document No. 2005-01-2279. <http://papers.sae.org>/2005-01-2279; 2005.

[3] Kirby R. Modeling sound propagation in acoustic waveguides using a hybrid model numerical method. J Acoust Soc Am 2008;124(4):1930–40.

[4] Craggs A. The application of the transfer matrix and matrix condensation methods with finite elements to duct acoustics. J Sound Vib 1989;132(2):393–402.

[5] Allard JF, Atalla N. Propagation of sound in porous media. 2nd ed. UK: John Wiley & Sons Ltd.; 2009.

[6] Munjal ML. Acoustics of ducts and mufflers. New York: Wiley-Interscience; 1987.

[7] Gerges SNY, Jordan R, Thieme FA, Bento Coelho JL, Arenas JP. Mufflers modeling by transfer matrix method and experimental verification. J Braz Soc Mech Sci Eng 2005;XXVII(2):132–40.

[8] Sahasrabudhe AD, Anantha Ramu S, Munjal ML. Matrix condensation and transfer matrix techniques in the 3-D analysis of expansion chamber mufflers. J Sound Vib 1991;147(3):371–94.

[9] Kim JT, Ih JG. Transfer matrix of curved duct bends and sound attenuation in curved expansion chambers. Appl Acoust 1999;56:297–309.

[10] Panigrahi SN, Munjal ML. Plane wave propagation in generalized multiply connected acoustic filters. J Acoust Soc Am 2005;118(5):2860–8.

[11] Tao Z, Seybert AF. A review of current techniques for measuring muffler transmission loss. In: SAE 2003 noise & vibration conference and exhibition (Grand Traverse, MI). Document No. 2003-01-1653, <http://papers.sae.org>/2003-01-1653; 2003.

[12] Munjal ML, Doige AG. Theory of a two source-location method for direct experimental evaluation of the four-pole parameters of an aeroacoustic element. J Sound Vib 1990;141(2):323–33.

[13] Allard J-F, Brouard B, Lafarge D, Lauriks W. Reciprocity and antireciprocity in sound transmission through layered materials including elastic and porous media. Wave Motion 1993;17:329–35.

[14] Morand H, OhayonR. Interactions fluids structures. Masson, Paris; 1992.

[15] Geebelen N, Boeckx L, Vermeir G, Lauriks W, Allard J-F, Dazel O. Measurement of the rigidity coefficients of a melamine foam. Acta Acust Acust 2007;93:783–8.